

THE DISTRIBUTION OF DARK MATTER IN A RINGED GALAXY

A. C. Quillen^{1,2,3} & J. A. Frogel^{4,5}

ABSTRACT

Outer rings are located at the greatest distance from the galaxy center of any feature resonant with a bar. Because of their large scale, their morphology is sensitive to the distribution of the dark matter in the galaxy. We compare periodic orbits integrated in the ringed galaxy NGC 6782 near the outer Lindblad resonance to the shape of the outer ring. The non-axisymmetric component of the potential resulting from the bar is derived from a near-infrared image of the galaxy. The axisymmetric component is derived assuming a flat rotation curve. We find that the maximally pinched non-self-intersecting periodic orbits are more elongated for higher bar mass-to-light ratios. For the orbits to be consistent with the observed ring morphology the mass-to-light ratio of the bar must be high and so a maximal disk value is preferred. This implies that either there is little dark matter within the bar, or that the dark matter contained in the disk of the galaxy is non-axisymmetric and rotates with the bar.

Subject headings: galaxies: kinematics and dynamics — galaxies: halos — galaxies: structure — galaxies: spiral

1. INTRODUCTION

Outer rings are located at the greatest distance from the galaxy center of any feature resonant with a bar. Because of their great distance from the galaxy center, their morphology should be sensitive to the distribution of the dark matter in the galaxy. Since they are resonant with the bar they are also sensitive to the mass-to-light ratio of the bar. These rings provide a unique opportunity to constrain the mass-to-light ratio of the luminous stellar matter in a galaxy, thus telling us about the dark matter distribution.

¹Astronomy Department, Ohio State University, 174 W. 18th Ave., Columbus, OH 43210

²University of Arizona, Steward Observatory, Tucson, AZ 85721

³E-mail: aquillen@as.arizona.edu

⁴Visiting Astronomer at Cerro Tololo Interamerican Observatories

⁵also at Department of Physics, University of Durham, Durham, England

Three classes of rings can be seen in normal barred galaxies. Nuclear rings located inside the bar, inner rings which envelop the bar, and outer rings which surround the bar. The simulations of Schwarz 1981 first demonstrated that outer rings develop in the ISM near the Outer Lindblad Resonance (OLR) of the bar. Outer rings are classified (following Buta & Crocker 1991) as R1-type or R2-type rings, where R2-type rings are oval and aligned parallel to the bar and R1-type rings resemble an oval with dimples at the points where the ring is closest to the bar. When the rings contain spiral structure, they are classified as pseudo-rings and are denoted R1' or R2' rings. The two types of rings have morphology closely related to the two families of closed orbits near the OLR (e. g. see Contopoulos & Grosbøl 1989 or Kalnajs 1991). The bar in these galaxies causes many stellar orbits in the plane of the galaxy to intersect themselves. Because gas can shock, it cannot remain in these orbits, so it collects in orbits that are near the periodic orbit families which are not self-intersecting (Schwarz 1981). For an excellent review on the properties of ringed galaxies see Buta & Combes 1996.

In this paper we examine the sensitivity of the ring shape of an R1' ringed galaxy to the mass-to-light ratio of the bar. The non-axisymmetric component of the gravitational potential is derived from a J band image of the galaxy. The morphology of the ring is compared to periodic orbits near the OLR for different bar mass-to-light ratios. Using this comparison we place limits on the mass-to-light ratio of the bar, and so on the distribution of the dark matter in the galaxy.

2. THE IMAGES OF NGC 6782

NGC 6782 is the best example of an R1-type ringed galaxy found to date in the OSU galaxy survey. In a catalog of southern ringed galaxies (Buta 1995) the galaxy is classified as R1/SB(r)0/a. Buta 1995 shows this galaxy as a nice example of an R1' ringed galaxy and demonstrates that the outer ring is prominent in a $B - I$ color map and so is quite blue. Byrd et al. 1994 show NGC 6782 as an example of a galaxy that resembles their slow pattern speed simulations. The R1' ring in NGC 6782 has a radius of $\sim 60''$ which corresponds to 15kpc assuming a distance to the galaxy of 50 Mpc ($H_0 = 75 \text{ km s}^{-1} \text{ Mpc}^{-1}$).

The galaxy was observed in the near infrared J, H and K bands and in the visible B, V and R bands. These data are a preliminary part of a survey being carried out at the Ohio State University of ~ 220 galaxies (Frogel et al. 1996). The survey's goal is to produce a library of photometrically calibrated images of late-type galaxies from 0.4 to $2.2\mu\text{m}$. For notes on the observation and reduction techniques see Pogge et al. 1996, or for individual examples Quillen et al. 1994, and Quillen et al. 1995. All the images were observed at the Cerro Tololo Interamerican Observatories. The BVR images were observed at the 0.9m telescope on 1995 October 25 using the Tek#2 1024×1024 pixel CCD with a spatial scale of $0''.40/\text{pixel}$. Total on source exposure times were 30, 15 and 10 minutes for B, V and R respectively. The JHK images were observed at the 1.5m telescope on 1995 October 31 and 1995 Nov 2 using the NICMOS 3 256×256 pixel infrared array with a spatial scale of $1''.16/\text{pixel}$. Total on source exposure times were 15 minutes

at J and H and 29 minutes at K band. The infrared images were observed during photometric conditions and were calibrated on the CTIO/CIT system using standard stars listed by Carter & Meadows 1995. The optical images were observed during clear but non-photometric conditions.

Figure 1 shows B and J band images of the galaxy and an R/B color map. In the B band image (Figure 1a) the classic figure 8 shape of the R1-type ring can be seen. The ring has some spiral structure which causes the ring to be brighter on its north-east and south-west sides than on its north-west and south-east sides. This means that the ring does not have perfect mirror symmetry about its major axis. The pinches near the bar ends can be more clearly seen in the brighter north-east and south-west sides of the ring.

3. THE FORM OF THE GRAVITATIONAL POTENTIAL

To integrate orbits in the plane of the galaxy we require an estimate of the gravitational potential. We assume that the potential in the plane $\Phi(r, \theta)$ is a sum of two components, an axisymmetric one, $\Phi_0(r)$, and a component $\Phi_2(r)$ proportional to $\cos 2\theta$,

$$\Phi(r, \theta) = \Phi_0(r) + \Phi_2(r) \cos(2\theta) \quad (1)$$

where θ is the azimuthal angle in the plane of the galaxy and r is the radius. We take the bar to be aligned along the axis with $\theta = 0$.

3.1. The Axisymmetric Component

The axisymmetric component of the potential should be consistent with the rotation curve of the galaxy at the location of the outer ring. At the location of the outer ring in NGC 6782, dark matter is expected to contribute to the rotation curve. We therefore could not use a potential derived solely from the light distribution as did Quillen et al. 1994 & Quillen 1997 which were dynamical studies of bars in the central few kpc of galaxies.

Unfortunately, there is no published rotation curve for NGC 6782. Few ringed galaxies have measured rotation curves at large radii. However those few that have been observed, have rotation curves that are nearly flat. For example, the rotation curve of ESO-509-98 is very flat (Buta et al. 1996), and the HI velocity field shows the rotation curve of NGC 3351 to be nearly flat (A. Bosma private communication). Simulations of outer rings produce more realistic shaped rings in model galaxies with flat rotation curves (Byrd et al. 1994). In our orbit integrations, for the axisymmetric component of the potential, Φ_0 , we therefore assume a logarithmic form consistent with a flat rotation curve. Φ_0 is determined by one parameter, the circular velocity, which we estimate from the Tully-Fisher relation (see below).

Near infrared images are superior to visible images for dynamical studies because of their reduced sensitivity to extinction from dust and because they are dominated by light from an older

cooler stellar population that is more evenly distributed dynamically and a better tracer of the stellar mass in the galaxy than the bluer, hotter stars (e.g. Frogel 1988; Frogel et al. 1996). We use the J band image to determine the gravitational potential due to the luminous stellar component of the galaxy. The J band image was used because the sky is flatter outside the bar than it is in the H band image and because it has higher signal to noise than the K band image. The color $J - K = 1.0 \pm 0.05$ is constant across the bar, though the bulge of the galaxy ($r < 7''$) is redder with $J - K = 1.06 \pm 0.05$. The height of the rotation curve from the luminous stellar matter (traced in J band) allows us to define a maximal disk, and show that at the ring a significant dark component is needed to have a realistic flat rotation curve.

3.2. Galaxy Inclination

Before the gravitational potential due to luminous stellar matter can be generated from the infrared image, we must correct for the inclination of the galaxy. A statistical study of R1' ringed galaxies found that these rings have observed axis ratios of $q_0 = 0.74 \pm 0.08$ and position angles on the sky with respect to the bar of $\theta_0 = 90^\circ \pm 9^\circ$ (Buta 1995). Buta 1995 found that R1' rings are very nearly perpendicular to the bar and are elongated. Gas simulations of these rings support Buta 1995's finding for the ring alignment (Byrd et al. 1994). We therefore assume that the ring is perpendicular to the bar. This assumption reduces the degrees of freedom so that the major axis position angle is fixed by a choice for the inclination of the galaxy.

Another constraint on the galaxy inclination is obtained from the outermost detected isophotes. We constructed a sum of the B, V and R images weighted inversely by the noise in each band so as to maximize signal to noise in the outer regions of the galaxy. An outer isophote is displayed in Figure 1d. This isophote has major axis oriented at a position angle of $\sim 45^\circ$ and has an ellipticity of ~ 0.9 . This suggests that the galaxy is not highly inclined. Since early-type galaxies are less often warped than late-type galaxies (Bosma 1991), it is unlikely that the galaxy is warped at large radii. We therefore corrected for the inclination, i (where a face-on galaxy has $i = 0^\circ$), of the galaxy using various inclinations and their accompanying position angles (see Table 1). Deprojected images of the galaxies at these inclinations are shown in Figure 2.

The inclination $i = 41^\circ$ causes the ring in the plane of the galaxy to be rounder or to have a larger axis ratio than for $i = 35^\circ$. Inclinations higher than 45° cause the outer isophotes of the galaxy (see Figure 1d) to be very elliptical, or have an axis ratio less than 0.8 (see Table 1 for axis ratios). These outer isophotes are not aligned with any feature in the galaxy so they should be close to circular. Inclinations higher than 45° also cause the ring to be either aligned parallel to the bar or to be almost round (for $i = 49^\circ$, the ring axis ratio is ~ 1.0). This would be inconsistent with the statistics of R1' rings compiled by Buta 1995. For inclinations lower than 35° , the bar and the ring cannot be perpendicular. It is therefore unlikely that the inclination of the galaxy is outside the range $35^\circ < i < 45^\circ$.

After correcting for inclination, the gravitational potential in the plane of the galaxy traced by the luminous stellar matter was determined by convolving the J image of NGC 6782 with a function that depends on the vertical structure of the disk (Quillen et al. 1994). Before convolution stars were removed from the J image. The disk is assumed to have density $\propto \text{sech}(z/h)$ (following van der Kruit 1988) where z is the height above the plane of the galaxy and h is the vertical scale height. The resulting potential is insensitive to the choice of vertical function for functions such as sech , sech^2 and exponential with equivalent $\langle z^2 \rangle$ (Quillen 1996). Since the galaxy is distant, a small vertical scale height was used $h = 0''.5$. Quillen 1996 found that doubling the vertical scale height results in raising the Φ_2 component of the gravitational potential by $\sim 10\%$. We have deliberately made h small because the seeing in the images causes artificial smoothing equivalent to increasing the size of h .

3.3. What Do We Mean by a Maximal Disk?

Figure 3 shows the rotation curve derived from the axisymmetric component of the potential generated from the J image for the different galaxy inclinations. The horizontal line shown in Figure 3 is the circular rotational velocity computed using the Tully-Fisher Relation. For an H band total magnitude of 8.87 measured from our H band image, we compute a circular velocity of 320 km s $^{-1}$ using the relation given in Pierce & Tully 1992. All subsequent values given in this paper will be in units with respect to this circular velocity. This circular velocity is also what we used for the flat rotation curve axisymmetric component of the potential in our orbit integrations at the location of the ring. The rotation curves shown in Figure 3 assume a distance of 50 Mpc ($H_0 = 75$ km s $^{-1}$ Mpc $^{-1}$) to the galaxy and a mass-to-light ratio of $M/L_J = 1.23 \left(\frac{v_c}{320 \text{ km s}^{-1}} \right)^2 \left(\frac{50 \text{ Mpc}}{D} \right)$ or using the color of the bar $M/L_K = 0.69 \left(\frac{v_c}{320 \text{ km s}^{-1}} \right)^2 \left(\frac{50 \text{ Mpc}}{D} \right)$ in solar units (see Worthey 1994) where L_J and L_K are the luminosities in the J , and K bands and v_c is the true circular velocity of the galaxy.

For a “maximal disk” the rotation curve is attributed as much as possible to be from the visible components so that the halo could have a hollow core. (Some authors call a “maximal disk solution” one with a smooth halo that extends into the nucleus of the galaxy). The mass-to-light ratio listed above for the disk is what we take to give a “maximal disk”. This mass-to-light ratio was chosen so that the rotation curve generated from the J band light reaches above the circular velocity predicted from the Tully-Fisher relation. Once the true circular velocity for the galaxy has been observed, the mass-to-light ratio for the maximal disk can be rescaled. Because the three dimensional nature of the bulge was not properly taken into account in estimating the potential, the rotation curve is higher (by 10 – 20%) than it should be in the central 0 – 20''. This is why we have chosen the mass-to-light ratio such that the rotation curve is somewhat higher than the circular velocity near the galaxy nucleus.

We note that the rotation curve generated from the light drops with increasing radius. At the

radius of the ring ($\sim 60 - 70''$ or $15 - 17\text{kpc}$), a significant fraction of the mass must be from dark matter. Matter outside of our image which we do not detect exerts a radial force outwards, so that the rotation curve predicted from starlight should be even lower at large radii than we show in Figure 3.

3.4. The Non-Axisymmetric Component of the Gravitational Potential

The non-axisymmetric component of the potential should be due solely to the bar of the galaxy. Since the bar is in the disk of the galaxy, our inaccurate treatment of the bulge of the galaxy does not affect our measurement for $\Phi_2(r)$ (defined in equation 1). If luminous matter outside the image is axisymmetric then once again, our estimate for $\Phi_2(r)$ is not affected by neglecting this matter. This means that our orbit integrations which use only the Φ_2 component derived from the luminous matter are not affected by our inaccurate treatment of the bulge and outer disk. Higher order Fourier components of the potential are neglected since at the ring they are negligible.

The magnitude of the Φ_2 component measured from the potential due to luminous matter is shown in Figure 4 for the two inclinations assumed and for the maximal disk mass-to-light ratio discussed above. The Φ_2 component drops off quickly with radius as expected for a quadrupolar potential term. Also shown in Figure 4, an exponential function

$$\Phi_2(r) = A \exp(-r/a), \quad (2)$$

was fit to these Φ_2 components. The numerical values for these fits are listed in Table 1. These numbers show the strength of the non-axisymmetric component of the potential from the bar for the maximal disk, (corresponding to the rotation curves shown in Figure 3). For the higher inclinations Φ_2 component is substantially stronger because the bar becomes longer once deprojected. The exponential scale length of Φ_2 , a , is also larger for the higher inclination case (see Table 1). In the next section we discuss the effect of changing the disk mass-to-light ratio (and so the bar strength) on the morphology of the R1' ring.

4. MODELING THE RING

We integrate orbits in the plane of the galaxy for a gravitational potential with axisymmetric component consistent with a flat rotation curve and circular velocity determined from the Tully-Fisher relation. The non-axisymmetric component of the potential is derived from exponential fits to the Φ_2 components generated from the J band image for the two galaxy inclinations assumed. In our integrations we vary the strength of the bar by adjusting the mass-to-light ratio of the J band image and by keeping the circular velocity fixed. What we call the maximal disk corresponds to the mass-to-light ratios for the rotation curves shown in Figure 3 and the Φ_2 components

shown in Figure 4 with fitting parameters listed in Table 1. Varying the mass-to-light ratio of the disk corresponds to multiplying Φ_2 by a constant that is less than 1. Since the maximal disk mass-to-light ratio is determined by our assumption for the circular velocity (see discussion above), our results are not affected by the fact that actual circular rotational velocity is not known. Periodic orbits (or orbits that are closed in the frame in which the bar is stationary) in the plane of NGC 6782 were found by numerical integration as in Quillen et al. 1994.

In Figure 5 we show periodic orbits near the OLR for the maximal disk for a galaxy inclination of 41° . We see that the inner periodic orbits are more pinched near the bar, and have a rounder appearance. The outer orbits are more elongated and less pinched near the bar. Points in Figure 5 (and subsequent figures) are shown at equal timesteps along the orbit so that the gas density in the orbit should be high in the pinches near the bar. As pointed out by Kalnajs 1991 the gas in the ring cannot be in an orbit that intersects itself or that has loops. We therefore primarily show orbits that are maximally pinched but are not self-intersecting.

The location of the ring is set by the pattern speed of the bar. We have therefore adjusted the pattern speed of the bar so that the most pinched non-self-intersecting orbits are located near the outer ring. This sets the radius of corotation just past the end of the bar. That this happens is good evidence that the rotation curve of the galaxy is indeed nearly flat. For the orbits shown in Figure 5a, the radius of corotation is $37.7''$ and the bar angular rotation rate or pattern speed is $33.9 \text{ Gyr}^{-1} \times \left(\frac{v_c}{320 \text{ km s}^{-1}} \right)$.

Figure 5 shows that the maximal disk provides a good fit to the morphology of the ring for a galaxy inclination of $i = 41^\circ$. In the following sections we explore the sensitivity of the ring morphology to the bar strength and the galaxy inclination.

4.1. Varying the Strength of the Bar

Figure 6 shows comparisons between maximally pinched non-self-intersecting periodic orbits at a galaxy inclination of $i = 41^\circ$. All figures compare an orbit shown in Figure 5a that has a maximal disk mass-to-light ratio with a similar orbit for a mass-to-light ratio that is 75% of the maximal disk value. Figure 6a shows the comparison for two bars with the same pattern speed. We note that the weaker bar has a rounder maximally pinched orbit. This orbit is sufficiently round so that it does not extend along the bar major axis to large enough radius to be consistent with the morphology of the ring.

To explore the role of the bar pattern speed, in Figures 6b and c we show a similar comparison to the maximally pinched orbit of Figure 5a but the weaker bar has angular rotation rate factors of 1.097 and 0.927 times the rate used in Figure 6a. We see that a slower bar (Figure 6b) causes the maximally pinched orbit to be large enough so that it is coincident with the ring along the bar minor axis, however it is more oval than the ring so that along the bar major axis the ring is within the orbit. Raising the bar angular rotation rate (Figure 6c) causes the maximally pinched

orbit to be at too small a radius to fit the ring along any direction. Non-maximally pinched orbits for this pattern speed and mass-to-light ratio (one is shown in Figure 6d) are insufficiently pinched to look like the ring.

To summarize, weakening the bar potential at the location of the ring (equivalent to decreasing the disk mass-to-light ratio) causes the maximally pinched orbits to be rounder than the observed ring. It is not possible to resolve the problem by varying the bar pattern speed.

4.2. Varying the Exponential Scale Length of Φ_2

Since the different galaxy inclinations have Φ_2 components with different exponential scale lengths (see Table 1) we investigated the effect of varying this parameter. Figure 7 shows a comparison of the maximal disk $i = 41^\circ$ maximally pinched orbit with a similar orbit integrated in a model that has an equivalent Φ_2 strength at $r = 60''$ but with an exponential scale length, a , that is twice as long. We see that the two orbits are almost identical in shape. We find that the shape of the maximally pinched orbit is far more sensitive to the bar strength or the strength of Φ_2 than its exponential scale length. We do however expect that the extent of the periodic orbit family might vary between the two models.

4.3. Changing the Galaxy Inclination

For a lower galaxy inclination $i = 35^\circ$ the strength of the Φ_2 component is about half as large at the location of the ring (see Figure 4) than for $i = 41^\circ$. As expected from the previous section it is not possible to match the ring morphology with the periodic orbits without increasing the mass-to-light ratio past what we have defined as the maximal disk value. Figure 8 shows a model with a large pattern speed that is too round. Figure 8 shows orbits integrated for a maximal disk mass-to-light ratio with a bar angular rotation rate of $33.3 \text{ Gyr}^{-1} \times \left(\frac{v_c}{320 \text{ km s}^{-1}}\right)$. The periodic orbits are too round to match the observed ring morphology.

It would be possible to have a stronger bar or a larger mass-to-light ratio with a more carefully estimated maximal disk value. For example if the rotation curve of the galaxy increases then the maximal disk value for mass-to-light ratio could be higher. The ring enveloping the bar which is quite blue (see Figure 1c) may contain a large gas mass. This would increase the strength of the non-axisymmetric component of the potential and so cause the periodic orbits near the OLR to be more elongated.

For higher galaxy inclinations, the outer ring becomes rounder and the bar lengthens (see Figure 2). Lower mass-to-light ratios are required to match the observed morphology of the ring. In Figure 9 we show periodic orbits for a galaxy inclination of 45° that resemble the morphology of the ring for a mass-to-light ratio that is 75% of the maximal disk value. Since the average

radius of the ring is larger for this galaxy inclination than for lower inclinations, the bar angular rotation rate must be lower. The bar angular rotation rate for the orbits shown in Figure 9a is $29.0 \text{ Gyr}^{-1} \times \left(\frac{v_c}{320 \text{ km s}^{-1}} \right)$ and the radius of corotation is $44.2''$, again outside the end of the bar as expected.

It is extremely unlikely that the galaxy inclination is much higher than 45° since at 50° the ring is almost round. (see Figure 2).

5. SUMMARY AND DISCUSSION

We have assumed the following in modeling the R1' outer ring in NGC 6782: 1) The bar is perpendicular to the ring. This allowed us to determine the position angle for a given galaxy inclination. 2) The ring morphology consists of gas in orbits near to the maximally pinched non-self-intersecting orbits at the Outer Lindblad Resonance. 3) The rotation curve is flat. 4) The Φ_2 non-axisymmetric component of the potential is only due to the bar as seen in the J band image (gas is neglected). 5) The maximal disk mass-to-light ratio is well estimated from the axisymmetric component of the J band generated potential.

We find that the shape of the maximally pinched non-self-intersecting periodic orbits at the OLR is affected by the strength of the non-axisymmetric component Φ_2 of the gravitational potential, but is insensitive to its exponential scale length. A stronger Φ_2 results in more elongated orbits.

Using the above assumptions, and comparing outer ring morphology of NGC 6782 with the maximally pinched non-self-intersecting periodic orbits we find that a maximal disk value for the mass-to-light ratio is required to match the ring morphology for a galaxy inclination of $i = 41^\circ$. In this case the halo has no mass in its core. For $i = 45^\circ$ we find a mass-to-light ratio of 75% of the maximal disk value is required. For $i = 35^\circ$ a value larger than the maximal disk value assumed here is required. A larger mass-to-light ratio could be allowed if a large gas mass is found in the ring enveloping the bar (increasing the Φ_2 component of the potential), or if the rotation curve rises near the ring.

Larger galaxy inclinations are unlikely for the following reasons: 1) The ring becomes round or aligned with the bar which is not supported by statistics of R1-type rings (Buta 1995). However, NGC 6782 could be a special case. 2) The outer isophotes of the galaxy become significantly elongated.

A measured rotation curve will enable us to place a value on the maximal disk mass-to-light ratio assumed here and check whether our assumption of a flat rotation curve is a good one. A measured rotation curve would also allow us to measure the core radius of the dark matter halo using our values for the mass-to-light ratio. Deeper images showing the shapes of the isophotes past the ring may help to constrain the inclination angle of the galaxy. We plan to observe the

velocity field of the ring and compare it to that predicted from the periodic orbits. We also plan to observe other ring galaxies to find if maximal disk models are required generally. Modeling of galaxies with different orientations should help resolve the uncertainties caused by projection.

Gas simulations of rings could be studied to discover how well closed orbits match the gas morphology in these systems, which particular orbits collect gas, and how close outer rings are to being perpendicular to their bars.

If a maximal disk value for the bar mass-to-light ratio is indeed required (as suggested here) then either the inner parts of galaxies have little dark matter, or the dark matter contained in the disk of the galaxy is non-axisymmetric and rotates with the bar. The second possibility implies that the “conspiracy of shapes” suggested by Sackett et al. 1994 extends into the bar, and would lend support to the idea that dark matter halos are flattened (Sackett et al. 1994; Olling 1996), since if the dark matter rotates, it should be flattened.

We acknowledge helpful discussions and correspondence with R. Buta, A. Gould, D. Weinberg, K. Griest, P. Sackett, G. Rieke & A. Bosma. The OSU galaxy survey is being supported in part by NSF grant AST 92-17716. A.C.Q. acknowledges the support of a Columbus fellowship and a grant for visitors from L’Observatoire de Marseille. J.A.F. thanks Roger Davies for his hospitality at Durham University and PPARC for partial support via a Visiting Senior Research Fellowship.

REFERENCES

- Bosma, A. 1991, in *Warped Disks and Inclined Rings around Galaxies*, eds S. Casertano et al., (Cambridge: Cambridge Univ. Press), 181
- Buta, R. 1995, *ApJS*, 96, 39
- Buta, R., & Combes, F. 1996, *Fundamentals of Cosmic Physics*, in press
- Buta, R., & Crocker, D. A. 1991, *AJ*, 102, 1715
- Buta, R., Lewis, M., & Purcell, G. B. 1996, in preparation
- Contopoulos, G., & Grosbøl, P. 1989, *Astronomy and Astrophysics Review*, 1, 261
- Byrd, G., Rautiainen, R., Salo, H., Buta, R., & Crocker, D. A. 1994, *AJ*, 108, 476
- Carter, B. & Meadows, V. 1995, private communication
- Frogel, J. A. 1988, *ARA&A*, 26, 51
- Frogel, J. A., Quillen, A. C., & Pogge, R. W. 1996, in *New Extragalactic Perspectives in the New South Africa*, ed. D. Block (Dordrecht: Kluwer), in press
- Kalnajs, A. J. 1991, in *Dynamics of Disk Galaxies*, ed. B. Sundelius, Göteborgs University and Chalmers University of Technology, Göteborg
- Olling, R. P. 1996, *ApJ*, in press
- Pierce, M. J., & Tully, R. B. 1992, *ApJ*, 387, 47
- Pogge, R. W., Quillen, A. C., DePoy, D. L., Frogel, J. A., Terndrup, D., Sellgren, K., Ramírez, S. V., Houdashelt, M., Tiede, G., Ali, B. Kuchinski, L., Davies, R., Canzian, B. 1996, in preparation
- Quillen, A. C., Frogel, J. A. & González, R. A. 1994, *ApJ*, 437, 162
- Quillen, A. C., Frogel, J. A., Kenney, J. D., Pogge, R. W., & DePoy, D. L. 1995, *ApJ*, 441, 549
- Quillen, A. C. 1996, page 157 “Spiral galaxies in the Near-IR”, *Proceedings of the ESO-MPA Workshop Held at Garching, Germany 7-9 June 1995*, eds D. Minniti and H.-W Rix, Springer-Verlag: Berlin Heidelberg
- Quillen, A. C. 1997, submitted to *ApJ*
- Sackett, P. D., Rix, H.-W., Jarvis, B. J., & Freeman, K. C. 1994, *ApJ*, 436, 629
- Schwarz, M. P. 1981, *ApJ*, 247, 77

van der Kruit, P. C. 1988, *A&A*, 192, 117

Worthey, G., 1994, *ApJS*, 95, 107

Fig. 1.— a) Grayscale B band image of NGC 6782 overlaid with contours of the bar 0.5 mag apart. The image is uncalibrated so we do not know the absolute scale. b) J band contours of the bar. The brightest contour is at $15.5 \text{ mag/arcsec}^2$ and the difference between contours is 0.5 mag/arcsec^2 . c) R/B color map similar to that shown by Buta 1995. d) Low surface brightness contour in an image that is a noise weighted sum of the B , V and R band images. Note the change in angular scale between this figure and the other figures. We note that this outer isophote is almost round suggesting that the galaxy is not highly inclined.

Fig. 2.— Deprojected B band images for the inclinations and position angles listed in Table 1. Note that the higher the galaxy inclination the rounder the ring and the longer the bar. The position angles have been chosen so that the bar is approximately perpendicular to the ring. a) $i = 35^\circ$ b) $i = 41^\circ$ c) $i = 45^\circ$ d) $i = 49^\circ$

Fig. 3.— The rotation curves from the axisymmetric component of the J band generated gravitational potential for a maximal disk using the mass-to-light ratio given in the text. Rotation curves for galaxy inclinations of $i = 35^\circ$ and 45° have been plotted as solid lines. There is little difference between them. The straight dotted line represents a flat rotation curve with a circular velocity of 320 km s^{-1} predicted using the Tully-Fisher relation. Once the true circular velocity, v_c , of the galaxy is observed, the mass-to-light ratio for the maximal disk should be rescaled. For a non-maximal disk the rotation curve resulting from the luminous stellar matter would be lower than that shown here.

Fig. 4.— The amplitude of the non-axisymmetric component Φ_2 of the J band generated gravitational potential for the maximal disk. The solid lines are for galaxy inclinations of $i = 45^\circ$, 41° and 35° in order of decreasing height. Once the true circular velocity, v_c , of the galaxy is observed, the mass-to-light ratio for the maximal disk should be rescaled. The dotted lines are exponential fits to these curves with strengths and scale lengths listed in Table 1.

Fig. 5.— a) Periodic Orbits near the Outer Lindblad Resonance with a maximal disk value for the mass-to-light ratio at a galaxy inclination of $i = 41^\circ$. Points are plotted at equal timesteps in the rotating frame in which the bar is still. b) Grayscale of the deprojected galaxy for $i = 41^\circ$. The maximal disk provides a good representation for the morphology of the ring.

Fig. 6.— The effect of the strength of the bar on the shape of the maximally pinched non-self-intersecting periodic orbits for a galaxy inclination $i = 41$. a) A maximally pinched non-self-intersecting orbit for the maximal disk (solid line) compared to a similar orbit for a weaker bar with a mass-to-light ratio that is 75% as large as the maximal disk value (open points). b) Same as in a) except the orbit from the weaker bar has a lower bar pattern speed. c) Same as in a) except the orbit from the weaker bar has a higher bar pattern speed. d) Same as in c) except that the orbit from the weaker bar is not maximally pinched.

Fig. 7.— The effect of increasing the exponential scale length of the non-axisymmetric component of the potential Φ_2 . A maximally pinched non-self-intersecting orbit for the maximal disk (solid line) at $i = 41^\circ$ compared to a similar orbit for Φ_2 which is the same strength at $r = 60''$ but with has an exponential scale length twice as long (open points). The orbits are almost identical in shape. The shape of the orbits primarily depends on the strength of Φ_2 not on its exponential scale length.

Fig. 8.— a) Periodic Orbits near the Outer Lindblad Resonance with a maximal disk value for the mass-to-light ratio at a galaxy inclination of $i = 35^\circ$. Points are plotted at equal timesteps. b) Grayscale of the deprojected galaxy for $i = 35^\circ$. The maximal disk produces maximally pinched orbits that are too round to be consistent with the morphology of the ring. A bar strength with a mass-to-light ratio larger than the maximal disk value assumed here would be required to match the ring morphology.

Fig. 9.— a) Periodic Orbits near the Outer Lindblad Resonance for a mass-to-light ratio that is 75% of the maximal disk value at a galaxy inclination of $i = 45^\circ$. This mass-to-light ratio provides a good representation for the morphology of the ring. b) Grayscale of the deprojected galaxy for $i = 45^\circ$.

Table 1. Galaxy Orientation and Exponential Fits to Φ_2

Inclination	PA ⁱ	$A(\text{km s}^{-1})^{2j}$	$a(\text{arcsec})^k$	Outer Axis Ratio ^l
35°	58°	3.78×10^4	17.5	1.0
41°	45°	3.51×10^4	22.5	0.83
45°	32°	3.63×10^4	24.3	0.76
49°	25°	3.40×10^4	26.3	0.70

ⁱGalaxy major axis Position Angle required for the bar to be perpendicular to the ring at the given inclination.

^jFor a maximal disk mass-to-light ratio (see equation 2). Once the true circular velocity, v_c , of the galaxy is known these numbers should be multiplied by $\left(\frac{v_c}{320\text{km s}^{-1}}\right)^2$.

^kExponential scale length of Φ_2 (see equation 2).

^lAxis ratio of the deprojected outer isophote shown in Figure 1d.

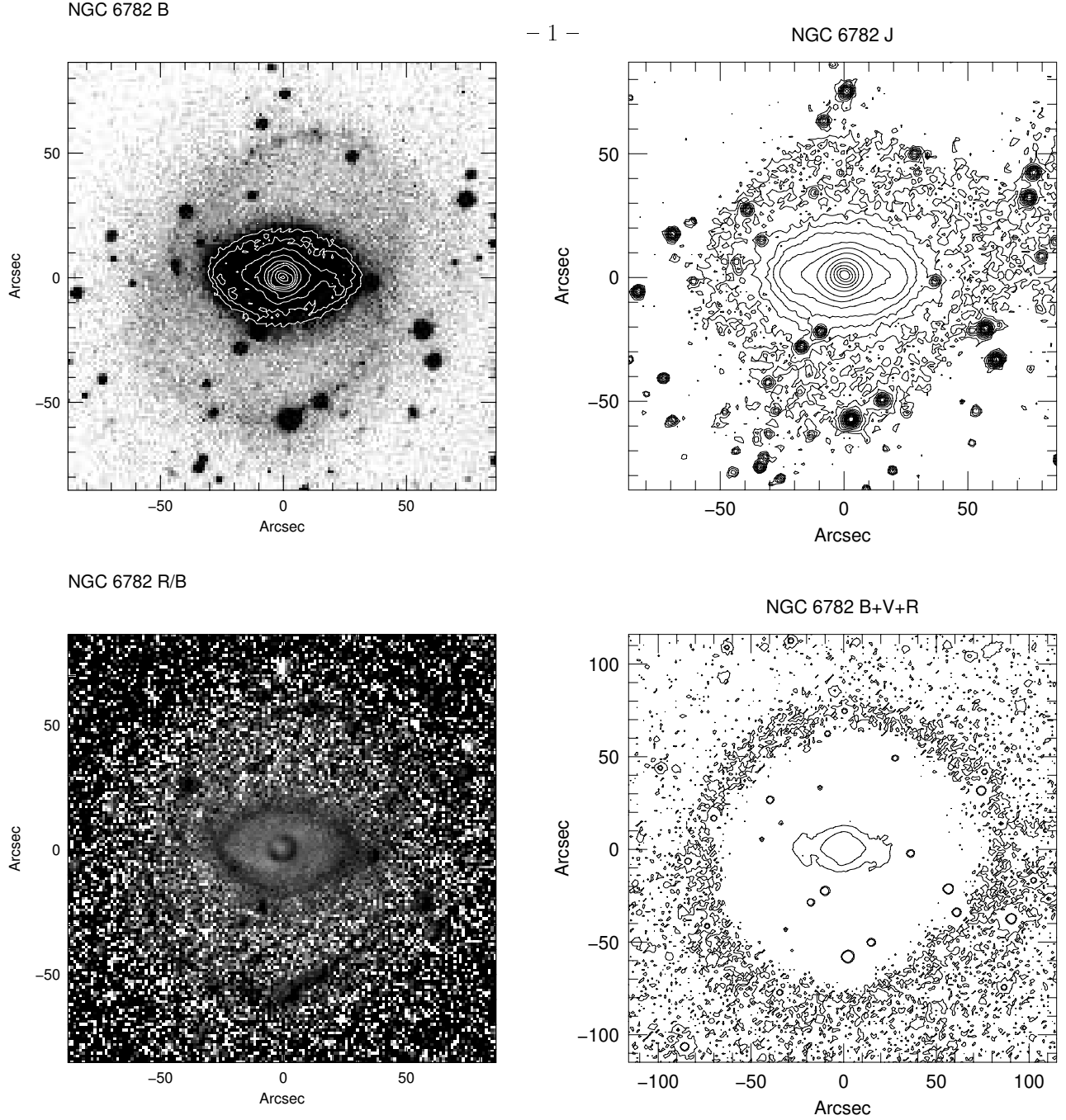
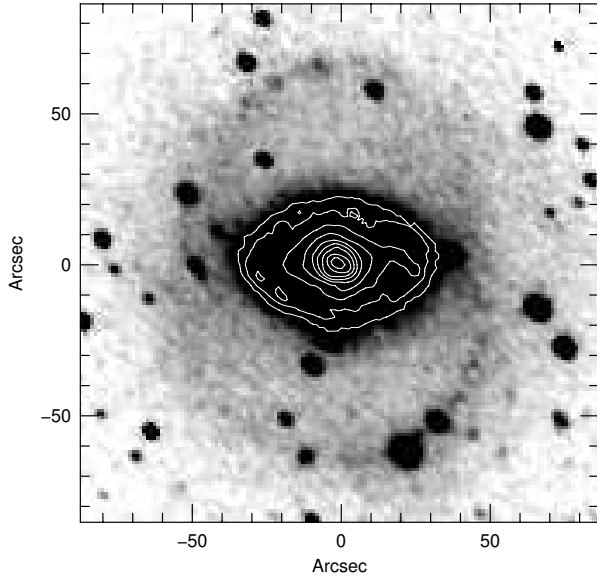


Fig. 1.— a) Grayscale B band image of NGC 6782 overlaid with contours of the bar 0.5 mag apart. The image is uncalibrated so we do not know the absolute scale. b) J band contours of the bar. The brightest contour is at $15.5 \text{ mag/arcsec}^2$ and the difference between contours is 0.5 mag/arcsec^2 . c) B/R color map similar to that shown by Buta 1995. d) Low surface brightness contour in an image that is a noise weighted sum of the B, V and R band images. Note the change in angular scale between this figure and the other figures. We note that this outer isophote is almost round suggesting that the galaxy is not highly inclined.

NGC 6782 B face-on $i=35$ 

- 2 -

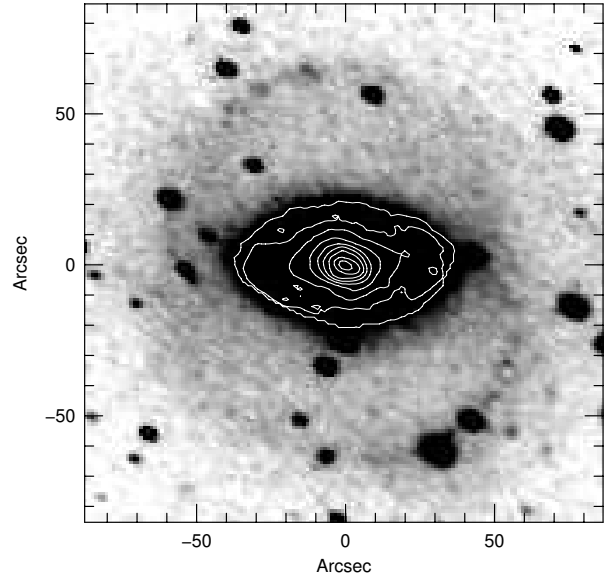
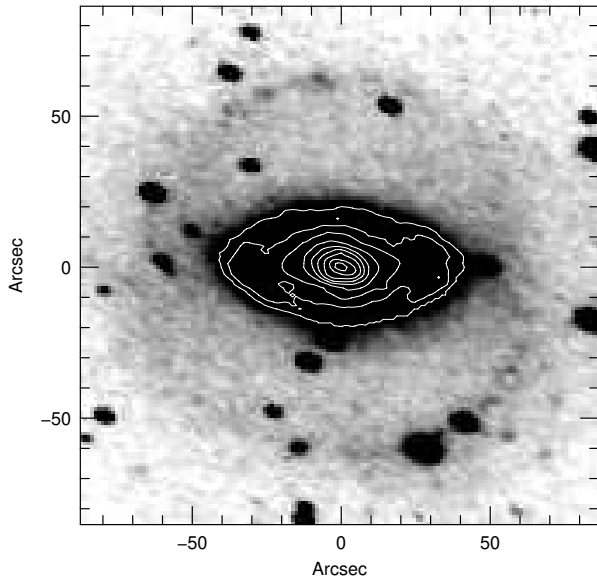
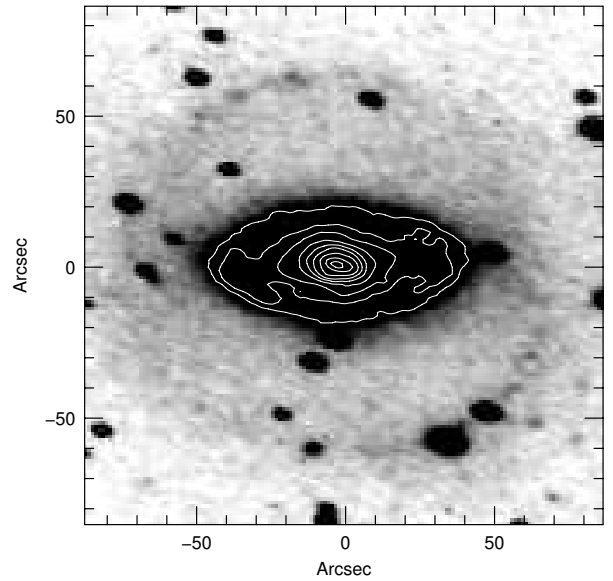
NGC 6782 B face-on $i=41$ NGC 6782 B face-on $i=45$ NGC 6782 B face-on $i=49$ 

Fig. 2.— Deprojected B band images for the inclinations and position angles listed in Table 1. Note that the higher the galaxy inclination the rounder the ring and the longer the bar. The position angles have been chosen so that the bar is approximately perpendicular to the ring. a) $i = 35^\circ$. b) Same as a) but for $i = 41^\circ$. c) Same as a) but for $i = 45^\circ$. d) Same as a) but for $i = 49^\circ$.

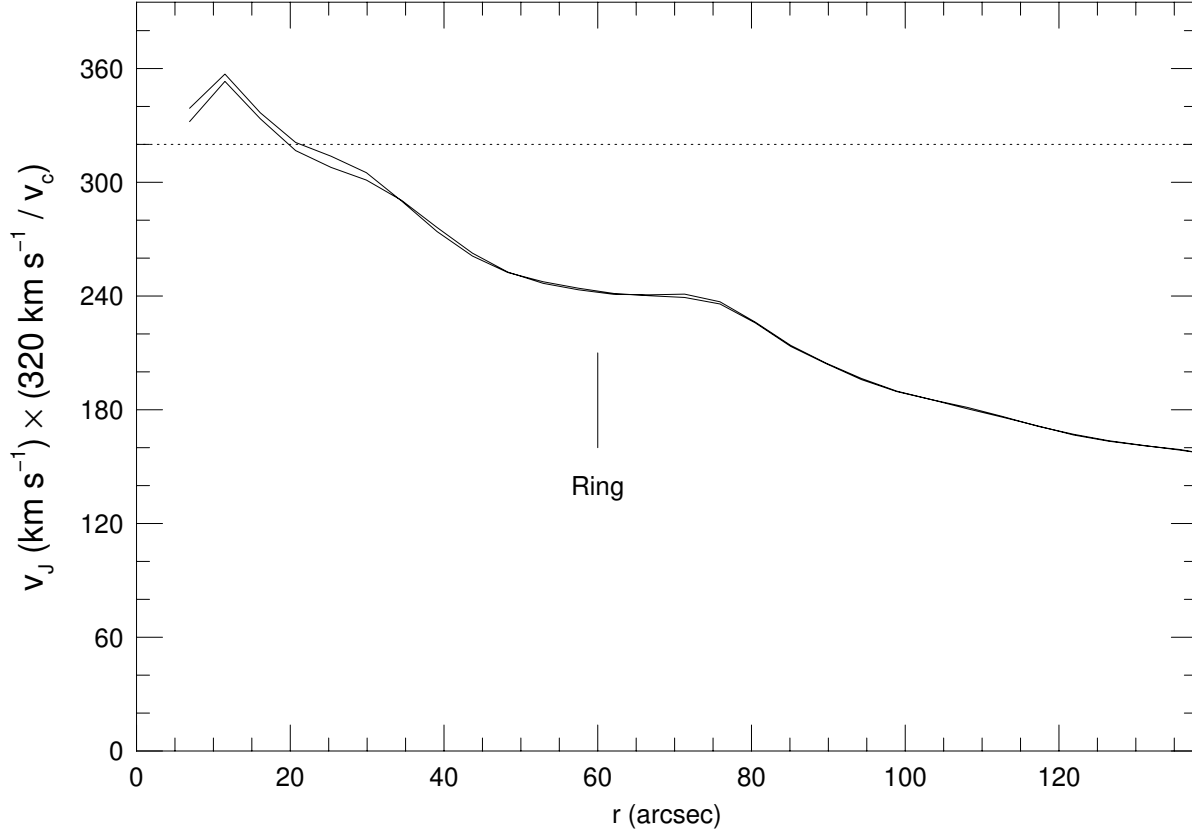


Fig. 3.— The rotation curves from the axisymmetric component of the J band generated gravitational potential for a maximal disk using the mass-to-light ratio given in the text. Rotation curves for galaxy inclinations of $i = 35^\circ$ and 45° have been plotted as solid lines. There is little difference between them. The straight dotted line represents a flat rotation curve with a circular velocity of 320 km/s predicted using the Tully-Fisher relation. Once the true circular velocity, v_c , of the galaxy is observed, the mass-to-light ratio for the maximal disk should be rescaled. For a non-maximal disk the rotation curve resulting from the luminous stellar matter would be lower than that shown here.

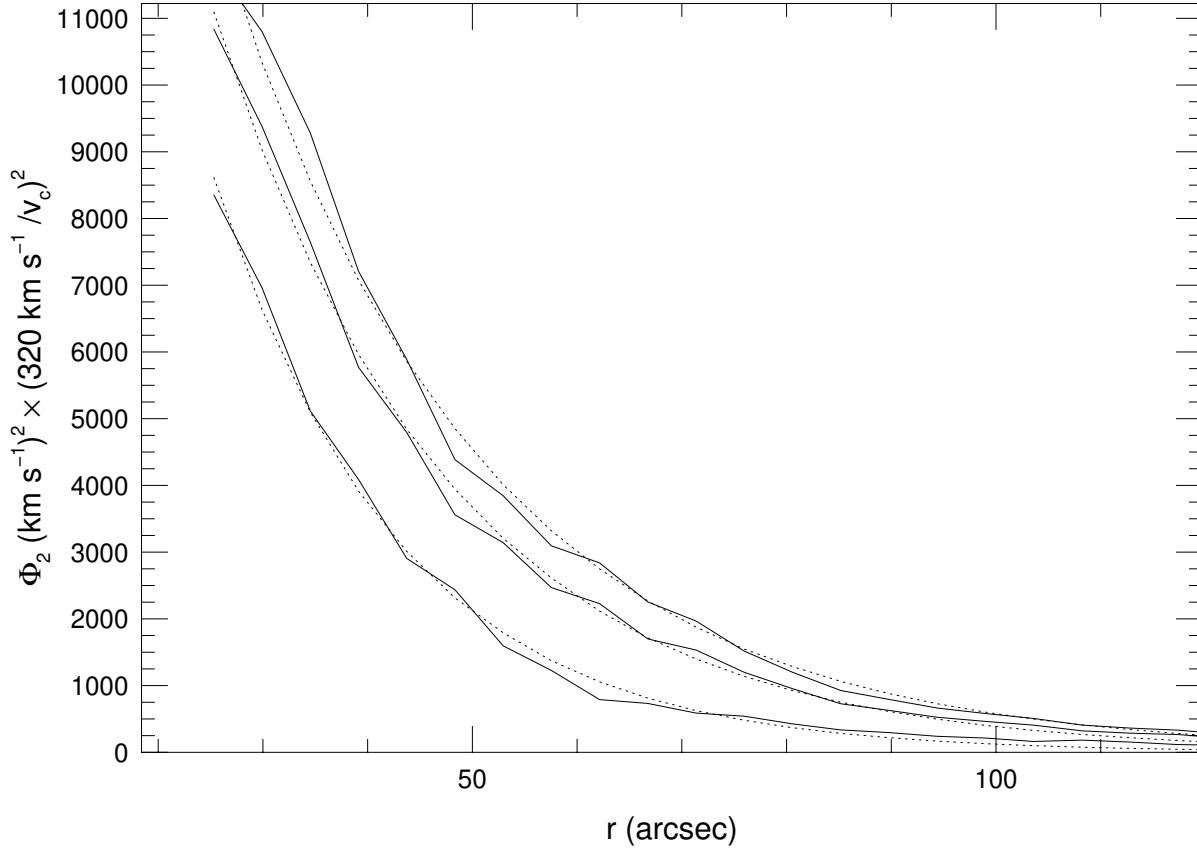


Fig. 4.— The amplitude of the non-axisymmetric component Φ_2 of the J band generated gravitational potential for the maximal disk. The solid lines are for galaxy inclinations of $i = 45^\circ$, 41° and 35° in order of decreasing height. Once the true circular velocity, v_c , of the galaxy is observed, the mass-to-light ratio for the maximal disk should be rescaled. The dotted lines are exponential fits to these curves with strengths and scale lengths listed in Table 1.

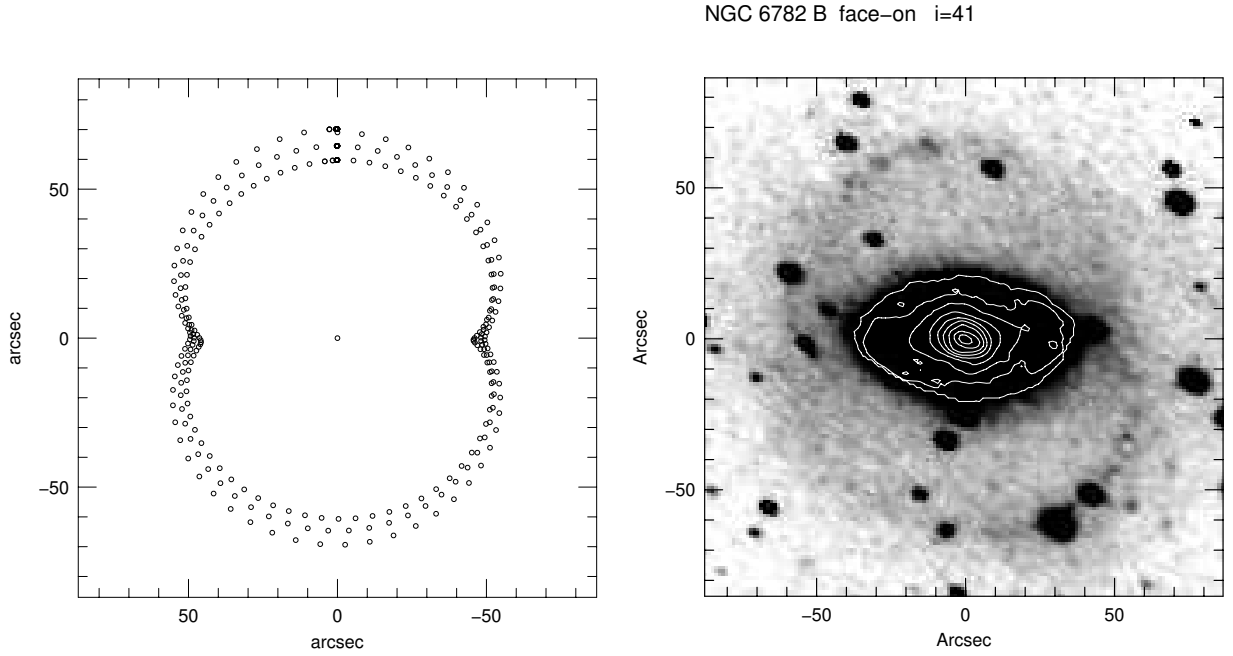


Fig. 5.— a) Periodic Orbits near the Outer Lindblad Resonance with a maximal disk value for the mass-to-light ratio at a galaxy inclination of $i = 41^\circ$. Points are plotted at equal timesteps in the rotating frame in which the bar is still. The maximal disk provides a good representation for the morphology of the ring. b) Grayscale of the deprojected galaxy for $i = 41^\circ$.

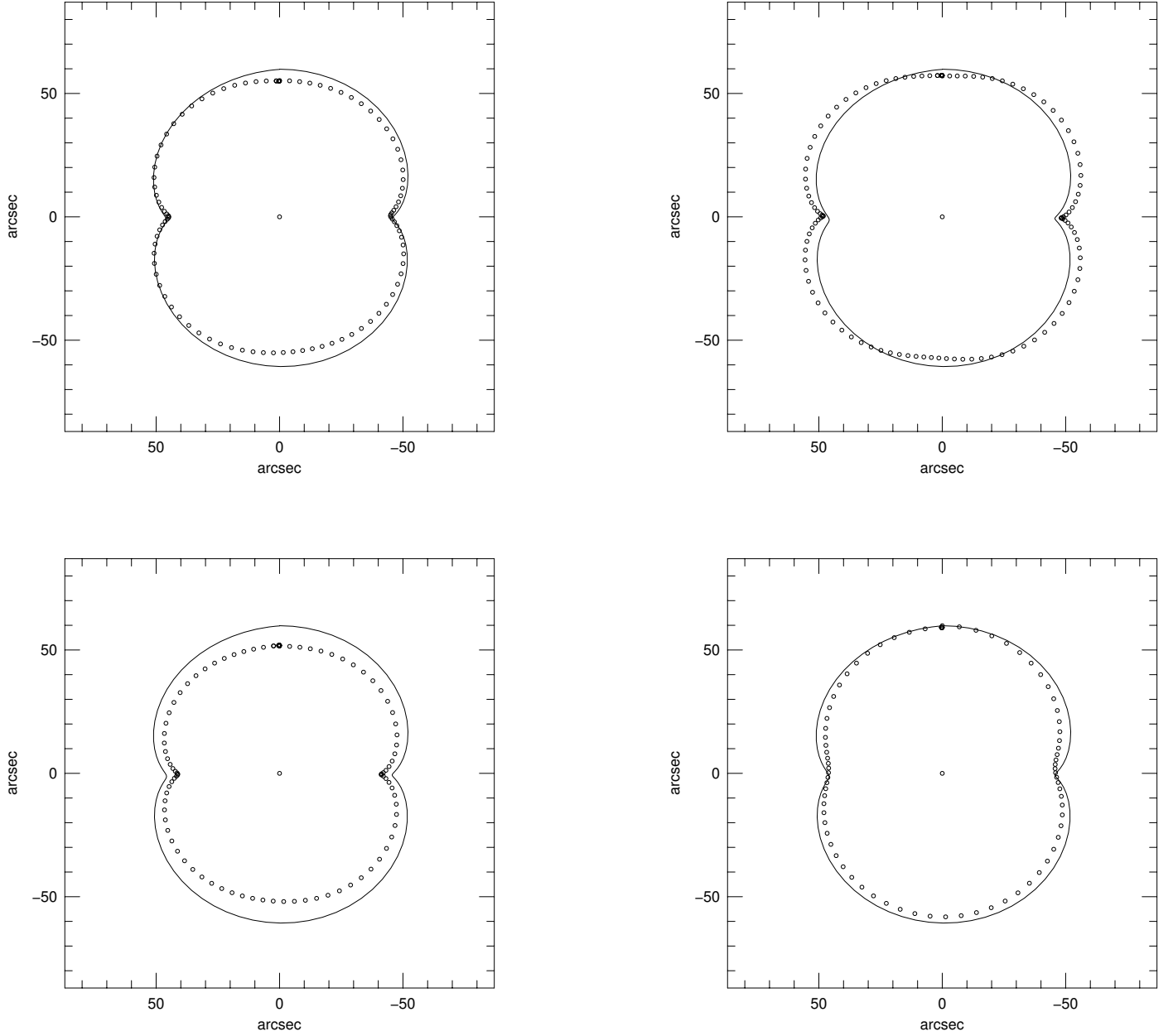


Fig. 6.— The effect of the strength of the bar on the shape of the maximally pinched non-self-intersecting periodic orbits for a galaxy inclination $i = 41$. a) A maximally pinched non-self-intersecting orbit for the maximal disk (solid line) compared to a similar orbit for a weaker bar with a mass-to-light ratio that is 75% as large as the maximal disk value (open points). b) Same as in a) except the orbit from the weaker bar has a lower bar pattern speed. c) Same as in a) except the orbit from the weaker bar has a higher bar pattern speed. d) Same as in c) except that the orbit from the weaker bar is not maximally pinched.

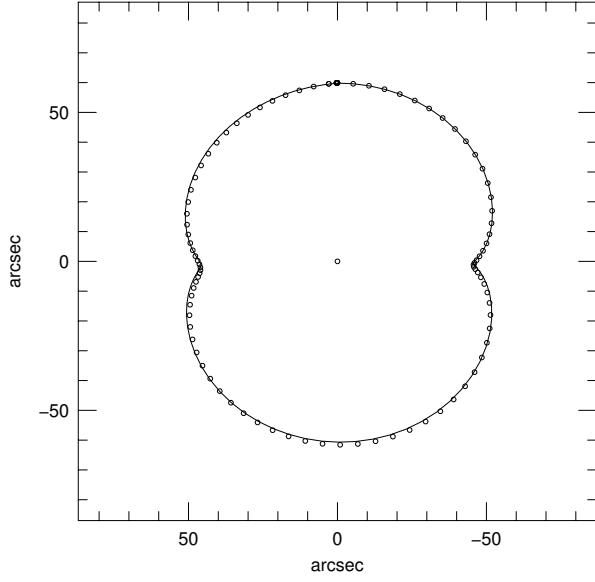


Fig. 7.— The effect of increasing the exponential scale length of the non-axisymmetric component of the potential Φ_2 . A maximally pinched non-self-intersecting orbit for the maximal disk (solid line) at $i = 41^\circ$ compared to a similar orbit for Φ_2 which is the same strength at $r = 60''$ but with has an exponential scale length twice as long (open points). The orbits are almost identical in shape. The shape of the orbits primarily depends on the strength of Φ_2 not on its exponential scale length.

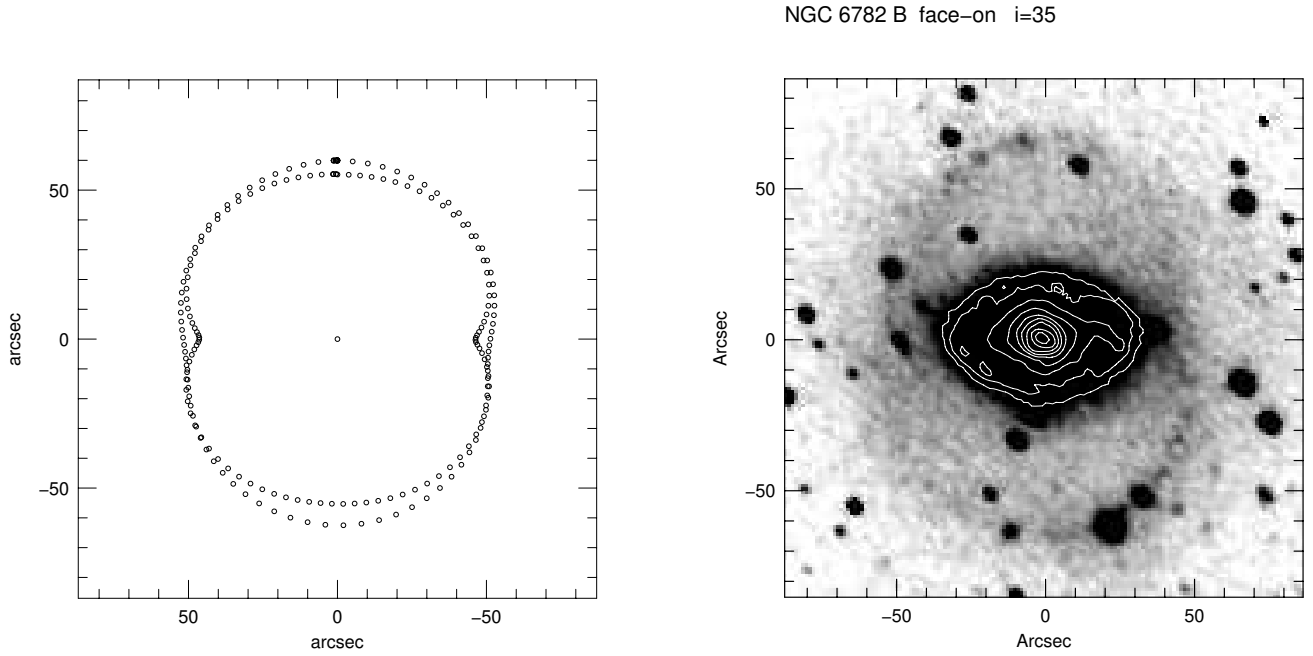


Fig. 8.— a) Periodic Orbits near the Outer Lindblad Resonance with a maximal disk value for the mass-to-light ratio at a galaxy inclination of $i = 35^\circ$. Points are plotted at equal timesteps. The maximal disk produces maximally pinched orbits that are too round to be consistent with the morphology of the ring. A bar strength with a mass-to-light ratio larger than the maximal disk value assumed here would be required to match the ring morphology. b) Grayscale of the deprojected galaxy for $i = 35^\circ$.

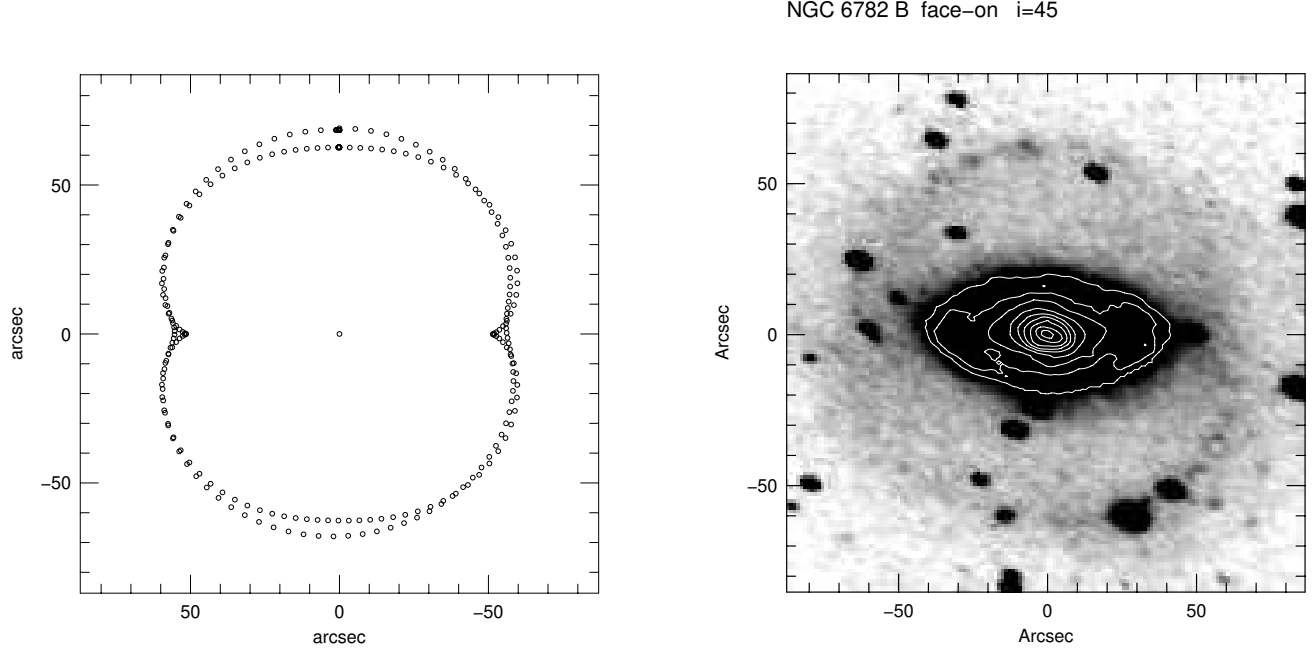


Fig. 9.— a) Periodic Orbits near the Outer Lindblad Resonance for a mass-to-light ratio that is 75% of the maximal disk value at a galaxy inclination of $i = 45^\circ$. This mass-to-light ratio provides a good representation for the morphology of the ring. b) Grayscale of the deprojected galaxy for $i = 45^\circ$.